

Article

Evaluation of Solar Conversion Efficiency in Dye-sensitized Solar Cells Using Natural Dyes Extracted from *Alpinia purpurata* and *Alstroemeria* Flower Petals as Novel Photosensitizers

Leonardo Ricardo Bernardes da Conceição ¹, Higor Oliveira da Cunha ¹, Arcano Matheus Bragança Leite ¹, Rajendran Suresh Babu ^{1,*}, Sebastian Raja ^{2,3}, Caue Ribeiro ^{2,3} and Ana Lucia Ferreira de Barros ¹

¹ Laboratory of Experimental and Applied Physics, Centro Federal de Educação Tecnológica Celso Suckow da Fonseca, Av. Maracanã 229, Rio de Janeiro 20271-110, Brazil; ana.barros@cefet-rj.br (A.L.F.d.B.)

² National Nanotechnology Laboratory for Agribusiness (LNNA), Embrapa Instrumentação, São Carlos 13560-970, Brazil; rajaorgchem@gmail.com (S.R.); caue.ribeiro@embrapa.br (C.R.)

³ Department of Chemistry, Federal University of São Carlos (UFSCar), São Carlos 13565-905, Brazil

* Correspondence: suresh.rajendran@aluno.cefet-rj.br; Tel.: +55-21-25663058

Abstract: Herein, we evaluate the conversion efficiency of dye-sensitized solar cells (DSSCs) photo-sensitized using two different natural dyes extracted from *Alpinia purpurata* and *Alstroemeria* flower petals. The appreciable absorption capacity of the extracts in the visible light region was examined through absorption spectroscopy. The functional groups of the corresponding pigments were identified through Fourier transform spectroscopy (FTIR) technique thus indicating the presence of cyanidin 3-glycosides and piperine in the flowers of *Alstroemeria* and *Alpinia purpurata*. The extracted dyes were immobilized on TiO₂ on transparent conducting FTO glass, which were used as photoanode. The dye-coated TiO₂ photoanode, Pt photocathode and iodide/triiodide redox electrolyte assembled into a cell module was illuminated by a light source intensity 100 mW/cm² to measure the photovoltaic conversion efficiency of DSSCs. The TiO₂ anode and Pt counter electrode surface roughness and morphological studies were evaluated using atomic force microscope (AFM) and field emission scanning electron microscopy (FESEM), respectively. Through the photoelectric characterizations, it was promising to verify that the solar conversion efficiency was calculated with the photovoltaic cell sensitized by *Alstroemeria* and *Alpinia purpurata*. This was achieved with a yield (η) of 1.74% and 0.65%, with an open-circuit voltage (V_{oc}) of 0.39 and 0.53 V, short-circuit current density (J_{sc}) of 2.04 and 0.49 mA/cm², fill factor (FF) of 0.35 and 0.40, and P_{max} of 0.280 and 0.100 mW/cm², respectively. The results are promising and demonstrate the importance of the search for new natural dyes to be used in organic solar cells for the development of devices that generate electricity in a sustainable way.

Keywords: dye-sensitized solar cells; natural dyes; photosensitizers; photovoltaics; renewable energy



Citation: da Conceição, L.R.B.; da Cunha, H.O.; Leite, A.M.B.; Suresh Babu, R.; Raja, S.; Ribeiro, C.; de Barros, A.L.F. Evaluation of Solar Conversion Efficiency in Dye-sensitized Solar Cells Using Natural Dyes Extracted from *Alpinia purpurata* and *Alstroemeria* Flower Petals as Novel Photosensitizers. *Colorants* **2023**, *2*, 618–631. <https://doi.org/10.3390/colorants2040032>

Academic Editors: Nadia Barbero, Carlotta Pontremoli and Simone Galliano

Received: 30 May 2023

Revised: 11 July 2023

Accepted: 13 September 2023

Published: 10 October 2023



Copyright: © 2023 by the authors. Licensee MDPI, Basel, Switzerland. This article is an open access article distributed under the terms and conditions of the Creative Commons Attribution (CC BY) license (<https://creativecommons.org/licenses/by/4.0/>).

1. Introduction

As global energy demand continues to grow, alternatives are being sought for the development of renewable, sustainable, proficient and inexpensive energy sources, for example solar power [1,2]. One of the ways to convert solar energy into electrical energy is through photovoltaic cells. Among these, this work deals with solar cells sensitized by dyes, which are called dye-sensitized solar cells (DSSCs). Michael Grätzel and O'Regan first developed DSSCs in 1991 at the École Polytechnique Fédérale de Lausanne [3]. The generation of electrical energy in these devices occurs through a process of electrochemistry between two electrodes through interactions between semiconductor oxides, such as TiO₂ and photosensitizing dyes, as well as with the application of an electrolytic solution between the anode and cathode capable of assisting the electric current from the oxidizing electrode to the Pt counter electrode. The dye molecules are in their ground state of low energy

(LUMO) prior to solar light incidence [3,4]. At present, the anodic surface of coated TiO₂ semiconductor oxide is subjected to the same energy level (near the valence band level), which is non-conducting [5]. When solar light falls on a DSSC device (oxidizing element), the molecules of dyes are excited and move from their lower energy ground state to a higher energy excited state (HOMO) [3–5]. In this way, the excited dye molecules have a higher energy level, overcoming the bandwidth difference of semiconductor valence band energy level. The photoexcitation of the dye with high absorption is essential for maximum use of sunlight incident on DSSCs [6].

DSSCs sensitized with commercial dyes containing heavy transition metal complexes, such as ruthenium-based complexes, are the most efficient, with power conversion efficiencies reaching as high as 11–12% when utilizing nanoporous TiO₂ electrodes [7,8]. However, ruthenium polypyridyl complexes contain a heavy metal that is harmful to the environment [9]. Furthermore, the high cost of ruthenium complexes and their long-term unavailability [10] shift the need to hunt for alternate photosensitizers for TiO₂-based photovoltaic devices. Natural dyes, on the other hand, can be used for the same purpose with good efficiency. Because of their huge absorption coefficients, high light-harvesting effectiveness, low cost, ease of preparation and environmental friendliness, researchers have recently concentrated on easily available dyes produced from natural sources as photosensitizers [11,12]. Natural dye pigments are present in different parts of a plant, including the flowers, fruits, leaves, stems and roots, and they are a potential alternative as photosensitizers for DSSC, but there are significant obstacles to be addressed before they can be used commercially on a large scale. The fundamental problems with dye conservation are its rapid degradation, lack of stability and limited lifespan. Despite the existence of coloring groups, they also have a smaller absorption spectrum, which lowers the effectiveness of photon capture. Among the natural dyes, flavonoids and anthocyanins stand out; this can be found in flowers and fruits [13]. These dyes have radiation absorption in the range of visible light, in the wavelength of 520 to 560 nm [14]. The absorption of anthocyanin on the surface of TiO₂ is only possible through the forces of Van der Waals, and it occurs through the bond between two atoms of anthocyanin oxygen with the Ti⁴⁺ ion found on the surface of TiO₂, with two bonds of unfilled positives [15]. The main electrochemical processes that occur in DSSCs are the separation and recombination of charges [16–19].

Recently, numerous natural pigments containing anthocyanin, betalains, chlorophyll, tannin and carotene have been successfully used as photosensitizers in DSSCs fabrication. For example, DSSCs constructed using dyes extracted from ivy gourd fruits and red frangipani flowers achieved an efficiency of 0.08% and 0.30%, respectively, in a study by Shanmugam et al. [20]. DSSCs have also been prepared from dye extracts of flame tree flower, pawpaw leaf and their mixture as photosensitizers. The anthocyanin extract of flame tree flower and chlorophyll extract of pawpaw leaves resulted in a DSSC of 0.20% efficiency each. The efficiency of solar conversion using their mixture reached an efficiency of 0.27%, and the mixed dye showed better conversion efficiency [21]. DSSCs fabricated using lemon extract (*Citrus limon*) showed an efficiency of 0.03% [22]. Dye extracted from cherry, blackberry, blueberry, raspberry and strawberry fruit when used as sensitizers in DSSC gave an efficiency of 0.21%, 0.69%, 0.21%, 0.20% and 0.14%, respectively [23]. Other natural dyes which are reported as sensitizers for DSSC are red Sicilian orange juice (*Citrus Sinensis*); purple extract of eggplant peels (*Solanum melongena*) [24]; pomegranate leaf and mulberry [25]; Siahkooti fruit [26]; fruit of *Melastoma malabathricum* [27]; bougainvillea flowers; red turnip; and the purple wild Sicilian prickly pear fruit juice [28]. DSSCs fabricated using extracts from *Nerium Oleander* (red-pink), *Bougainvillea* (dark pink), and *Hibiscus* (red) were found to give a conversion efficiency of 0.06%, 0.05% and 0.19%, respectively [29]. Precisely to meet the favorable conditions mentioned, the present research used the natural dyes extracted from the flowers of *Alpinia purpurata* and *Alstroemeria* rich in anthocyanin with a high capacity to absorb sunlight [30–32]. It should be noted that these flowers can be easily found in nature, unlike commercial inorganic dyes, such as ruthenium (Ru), which,

in addition to not being a photosensitizer compatible with the environment, also has a high cost [33].

In this work, we demonstrated low-cost new organic sensitizers extracted from *Alpinia purpurata* and *Alstroemeria* with a wide spectral range, in order to obtain good solar conversion efficiency. To the best of our knowledge, the dyes extracted from *Alpinia purpurata* and *Alstroemeria* flowers have not been previously employed as photosensitizer dye in DSSCs. The optical characteristics of the flower extracts were studied by FTIR spectroscopy and ultraviolet-visible (UV-Vis) spectroscopy. The surface morphology and topography of the photoelectrodes were examined using SEM and AFM, respectively. DSSCs using natural dye extracts as a photosensitizer from *Alpinia purpurata*- and *Alstroemeria*-coated TiO₂ were prepared, and the photoelectrical parameters provided by short-circuit current density (J_{SC}), open-circuit voltage (V_{OC}), fill factor (FF), power (P_{max}) and efficiency ($\eta\%$) were evaluated.

2. Experimental Section

2.1. Materials and Methods

To construct the photoelectrodes, a thin transparent film deposited on fluorine-doped tin oxide (FTO) was used and procured from Sigma-Aldrich and cut into desired size. Potassium iodide, polyethylene glycol, semiconductor TiO₂ (size \cong 20 nm) and chloroplatinic acid were also purchased from Sigma Aldrich. To avoid undesirable leaks from the junction between the anode and cathode, TEKBOND superglue was used. To evaluate the extracted natural dyes from the two flowers, Agilent Cary 630 FTIR (Santa Clara, CA, USA) and SHIMADZU UV-2600i spectrometers (Kyoto, Japan) were used. For annealing both electrodes, the QUIMIS Q318S25T muffle furnace (São Paulo, Brazil) was used. To examine the morphological and surface roughness of photoelectrodes, the JEOL JSM-7100F FESEM (Tokyo, Japan) and the Nanosurf Easyscan 2 atomic force microscope (Liestal, Switzerland) were used, respectively. The short-circuit (J_{SC}) and open-circuit voltage (V_{OC}) of each cell were obtained through the electrochemical characterizations carried out in the IVIUM Compactstat multi-potentiostat coupled to the Ivisun[®] IVIUM Technologies (Eindhoven, Netherlands), solar simulator using 100 mW/cm² of incident power.

2.2. Extraction of Dye

Fresh flowers of *Alpinia purpurata* and *Alstroemeria* were procured from a flower shop in Rio de Janeiro, Brazil. Before extracting the dyes, the flowers were cleaned with deionized water and the respective flower petals peeled and kept dried at room temperature. The dried petals were powdered mechanically; 10 g of dried powder was separated from the respective flowers and measured on the SHIMADZU ATY224 weighing balance (Barueri, Brazil). The dried powder was poured into 100 mL of ethanol solution in each beaker and soaked for 24 h. Finally, the extracted dyes were filtered through filter paper and kept in glass containers without any undesirable residues [34]. Finally, the dyes were stored in the refrigerator at a temperature of 5 °C in airtight containers and then used as photosensitizers in the construction of DSSCs.

2.3. Photoanode Fabrication

The TiO₂ photoanode was prepared by using the spin-coating method described elsewhere [34,35]: briefly, polyethylene glycol (0.3 g), powdered TiO₂ (1 g), distilled water (6 mL) and acetic acid (6 mL). The photoanode was prepared from the deposition of TiO₂ thin film on the FTO using a spin coater, with the speed controlled at 1000 rpm for a period of 10 s in order to obtain a homogeneous deposition. Finally, the electrodes were kept in the conventional oven annealed at 450 °C for 30 min and then steadily turned cold at ambient temperature.

2.4. Photocathode Fabrication

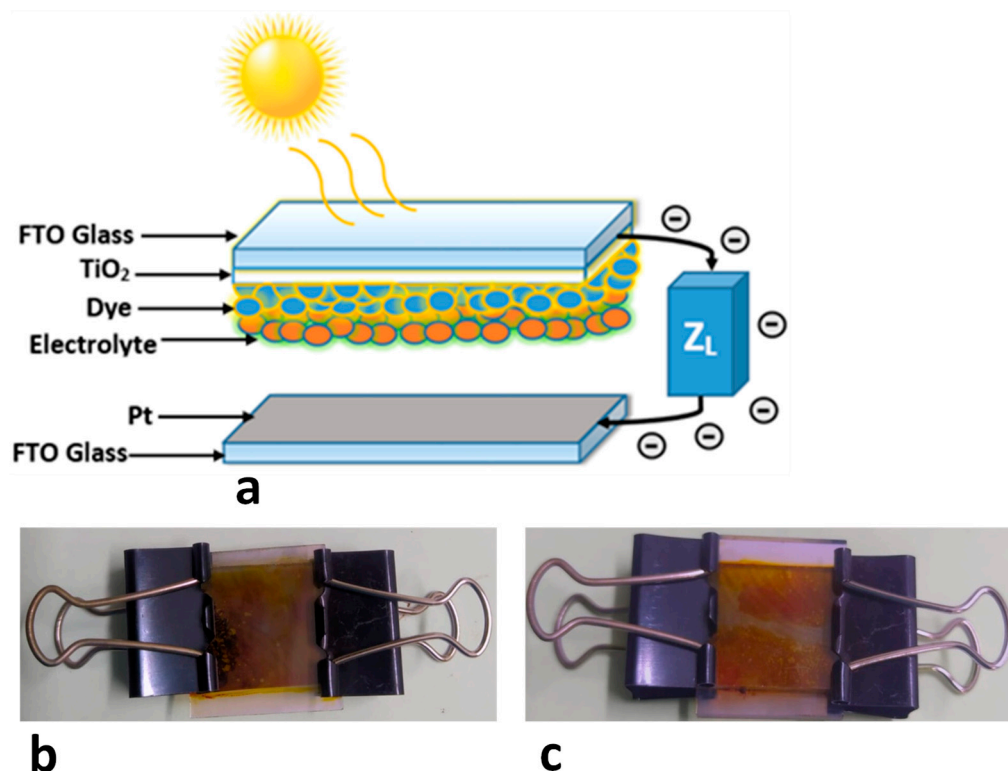
To minimize the errors caused by the resistance of the solar cell in controlling the potential of the working electrode, platinum (Pt) was used as a counter electrode. Pt was chosen because comparative studies have already been carried out between it and graphite, and Pt proved to be more efficient in its catalytic process, interacting in a more profitable way with the oxidizing electrode [36,37]. The Pt counter electrode was prepared through a 5 mM ethanolic solution of hexachloroplatinic acid ($\text{H}_2\text{Cl}_6\text{PtH}_2\text{O}$) using the drop casting method. In the last step, the electrode was kept in the conventional oven and annealed at $350\text{ }^\circ\text{C}$ for thirty minutes.

2.5. Electrolyte Preparation

The redox electrolyte for analyzing the performance of the DSSCs was synthesized by the solution containing potassium iodide (2.075 g), iodine (0.12 g) and polyethylene glycol (0.02 g) in acetonitrile (5 mL) [38–40].

2.6. Construction of DSSCs

Scheme 1 presents the assembly of the DSSC developed in this work. On the coated faces of the electrode (sensitized anode and cathode), a small external band was cleaned, which served as a contact for the electrochemical characterization and was placed in equidistant positions. For sealing, a small amount of instant glue was applied on the two faces adjacent to the one that was used as a contact. Finally, the electrolyte was injected between the two faces, and the cathode and anode were joined together.



Scheme 1. (a) Schematic representation of DSSC assembly diagram, (b,c) fabricated devices of *Alpinia purpurata* and *Alstroemeria* dyes, respectively.

3. Results and Discussion

3.1. FTIR Spectroscopy

Figure 1 presents the identification of the functional groups of each dye through the transmittance spectra obtained by FTIR. Analyzing the graph from Figure 1a, it is possible to observe the hydroxyl functional group (O-H) present in 3313 cm^{-1} , which is due to the

presence of anthocyanin group, as most of the characteristic peaks are matched with the previous literature [41,42]. On the side, it is possible to see the wavenumber from 2857 cm^{-1} to 2932 cm^{-1} referring to the C-H group asymmetric stretching vibrations, this peak being characteristic of the anthocyanin base molecule, positively corroborating the effectiveness of good photosensitization in solar cells, which reveals the characteristic peaks of cyanidin 3-glycosides pigment in the dye sample [43]. The band between 1649 and 1608 cm^{-1} is ascribed to the stretching vibrations of -C=C- group in rings of benzene and alkenes. The small band located at 1241 cm^{-1} could correspond to -C-O-C- stretching vibrations mode. In the case of Figure 1b, FTIR demonstrated that the dye contains -C-N , aromatic -C=C , -C=O , ethers -C-O , and aliphatic -C-H [44]. The stretching vibration at 1637 cm^{-1} is attributed to amide -C=O group and the aromatic -C=C absorption at 1511 cm^{-1} and 1461 cm^{-1} . The sharp peaks at 2854 cm^{-1} and 2917 cm^{-1} indicate -C-H asymmetric stretching vibrations. Based on the results, it was confirmed that *Alpinia purpurata* extracted dye contains an alkaloid compound known as piperine. The FTIR spectra of the dyes extracted from *Alstroemeria* and *Alpinia purpurata* flower petals in the present work were matched with previous literature [43,44]. The general chemical structure of cyanidin 3-glycosides and piperine is shown in Scheme 2.

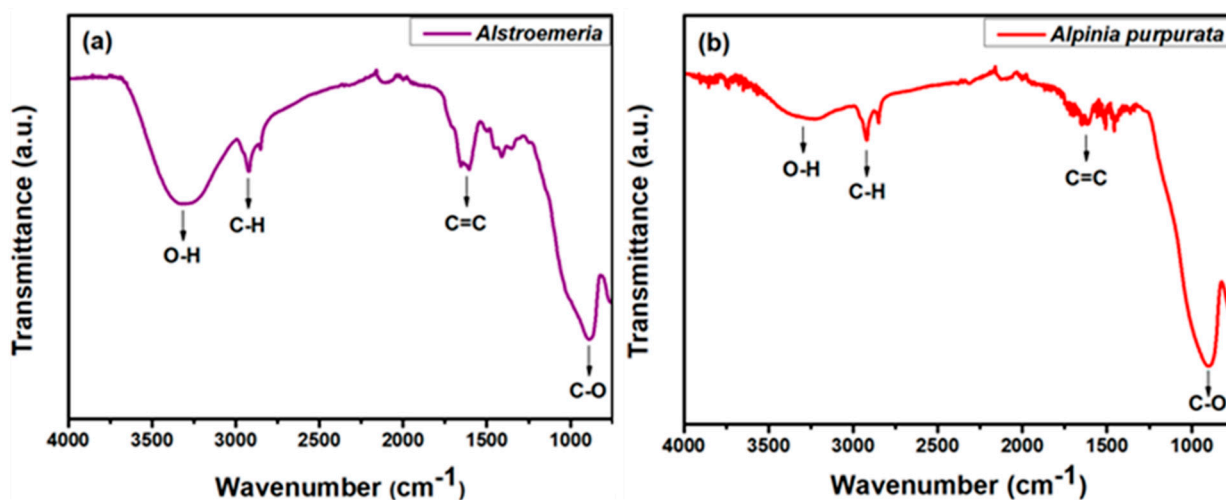
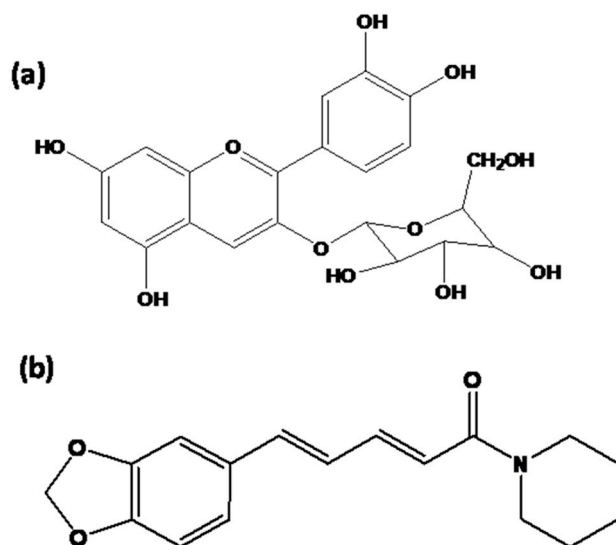


Figure 1. FTIR spectra of extracted dyes from: (a) *Alstroemeria* and (b) *Alpinia purpurata*.



Scheme 2. Molecular structure of cyanidin 3-glycosides (a) and piperine (b).

3.2. UV-Vis Spectroscopy

Through the wavelengths observed in the UV-Vis region, it is possible to evaluate the absorption transition between the ground state and excited state, as well as the amount of light energy absorbed by the molecules of the dyes. In the present study, ethanol was used as a solvent for the UV-Vis analysis of the *Alstroemeria* and *Alpinia purpurata* dyes. Figure 2a,b presents the absorption spectra of dyes extracted from the flowers of *Alstroemeria* and *Alpinia purpurata*. In Figure 2a, the peaks identified at 283 and 331 nm are the near visible range, which could be due to the absorption of pigments containing cyanidin 3-glycosides for the case of *Alstroemeria*. In Figure 2b referring to *Alpinia purpurata*, it was possible to observe a wide spectral range in the 267 and 342 nm peaks in the near visible range, which could be due to the absorption of pigments containing piperine. This region corresponds to the spectral range of the piperine and cyanidin 3-glycosides molecule, which is considered the main element present in organic dyes, in order to be used for photosensitization in solar cells [45]. The wavelengths specifically correspond to the compound cyanidin 3-glycosides anthocyanin radicals and piperine.

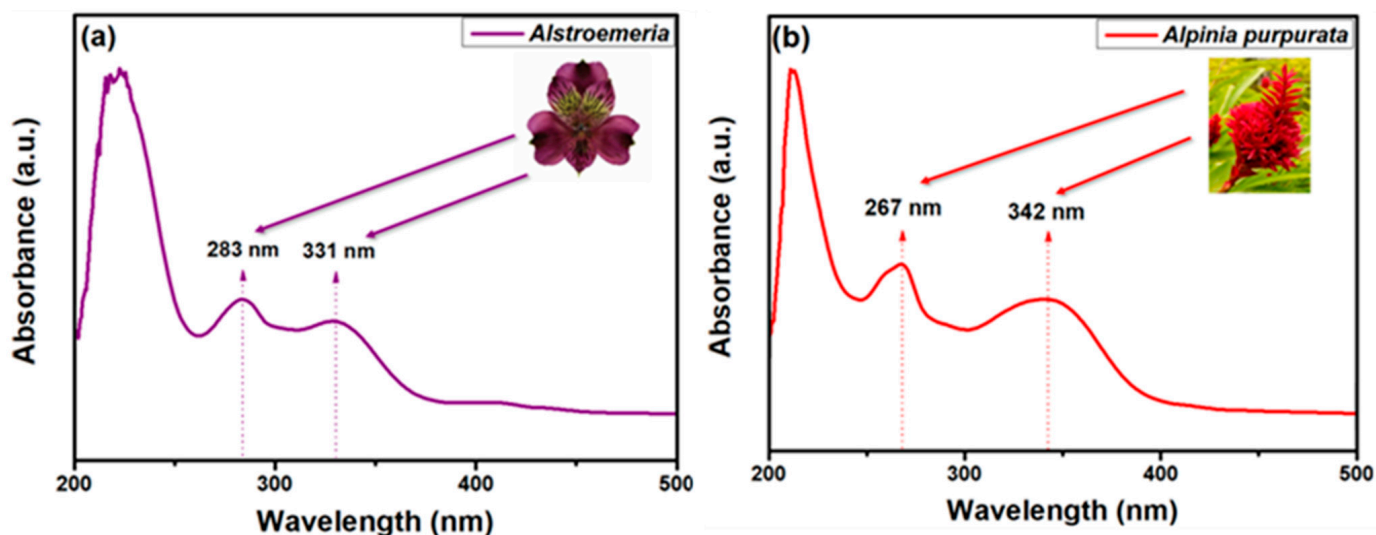


Figure 2. Absorption spectra of extracted dyes from: (a) *Alstroemeria* and (b) *Alpinia purpurata*.

3.3. FESEM

The size and morphologies of the TiO₂-deposited anode and Pt-deposited counter electrode, respectively, were obtained using SEM, as shown in Figure 3a,b. The semiconductor TiO₂ nanoparticles were homogeneously deposited on the FTO electrode surface. The particle sizes were ~20 to 30 nm (Figure 3a) and demonstrated that every TiO₂ nanoparticle was well connected with appropriate mesoporosity to permit an arrangement of a wide boundary of electrode/electrolyte. Further, the evaluation assigned that the electrode surface morphology is very rough and could be motivated to improving the adsorption of dye due to its high irregular surface and surface area. The thickness (depth profile) of the prepared TiO₂ electrode was ~6 μm, as shown in the inset of Figure 3a. Furthermore, the surface morphology of the nanostructured Pt cathode was performed as presented in Figure 3b. The surface morphology of photoanode showed a spherical-like structure of less than 50 nm with a small aggregation of Pt nanostructures. The Pt nanostructures improved the electrocatalytic activity and conductivity of the electron transfer in the photovoltaic performances in the DSSC device.

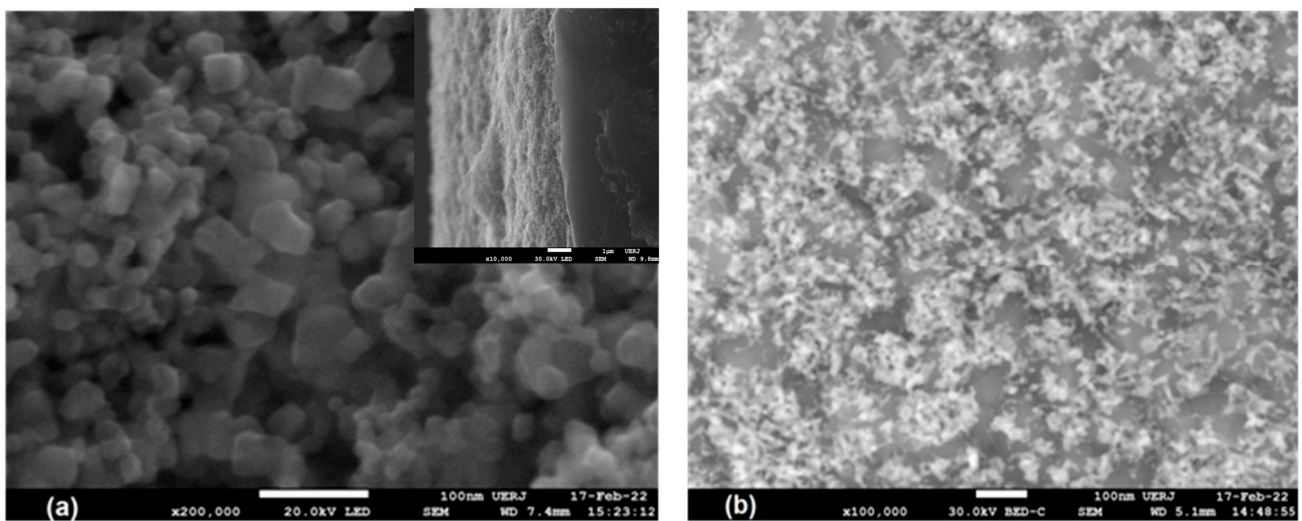


Figure 3. Morphological studies of (a) TiO₂ electrode and (b) Pt counter electrode.

3.4. AFM

The topography and surface roughness of the photoelectrodes were examined by 3-D AFM, as presented in Figure 4. The TiO₂ photoanode and Pt photocathode were examined by using a non-contact approach. The photoelectrode surface analysis (i.e., surface roughness) is the basic investigation of the elements, for example the semiconducting TiO₂ photoanode and platinum photocathodes performances. The presence of microporous structure and hollows plays a very important role in coating the semiconducting TiO₂ nanoparticles on the FTO surface, which should be mesoporous and uniform, coating the whole surface of electrode and exclusive of any fractures or big craters [46]. To attain the good performance of the DSSC, the TiO₂ coating should be completely uniform, which hinders the thin film and the possibility of recombination processes. However, to overcome this, various parameters are regulated, such as the sample preparation, coating method and regularity [47]. Furthermore, the DSSCs' efficiencies primarily depend on the components' construction method. Hence, optimizing each parameter is extremely significant to achieve higher efficiency. In DSSCs, the semiconducting TiO₂ electrode, as one of the main components, influences the photoelectric performances. Figure 4a shows that the surface TiO₂ photoelectrode was extremely homogeneous with expected root mean square (RMS) and a surface roughness of ~65 μm . Similarly, the photocathode was performed using the 3-D AFM, as presented in Figure 4b. The nanostructured Pt was homogeneously deposited on the surface of the FTO electrode, forming an excellent conducting cathode. The surface roughness (RMS) of the Pt counter electrode was 23 nm.

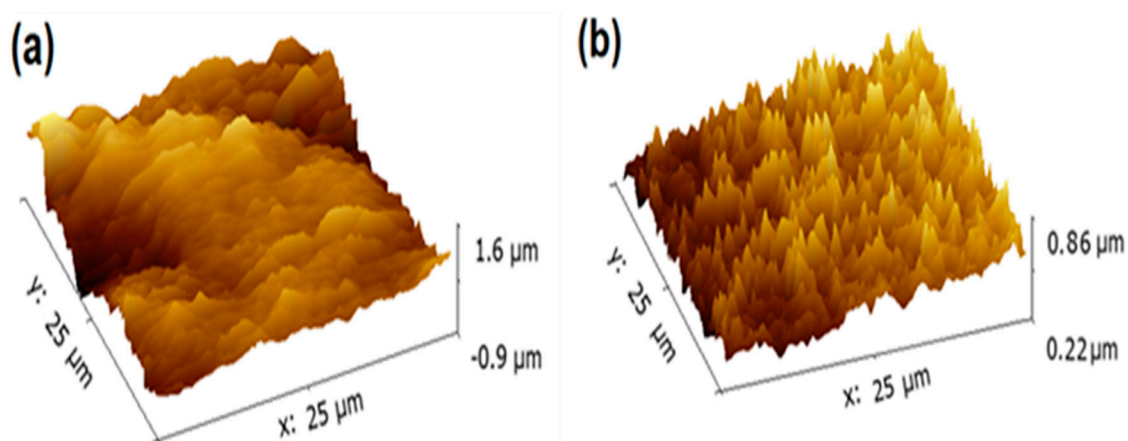


Figure 4. Surface topographical studies of (a) TiO₂ electrode and (b) Pt counter electrode.

3.5. Electrochemical Characterization

The prepared DSSCs were characterized electrochemically with a solar illumination of light intensity (100 mW/cm^2). The J - V curves of DSSCs were employed to obtain the photovoltaic parameters, such as short-circuit current density (J_{sc}), open-circuit voltage (V_{oc}), fill factor (FF), power maximum (P_{max}) and conversion efficiency (η). The efficiency (η) and FF were obtained from the below equations:

$$FF = J_{max} \times V_{max} / J_{sc} \times V_{oc} \quad (1)$$

$$\eta(\%) = J_{sc} \times V_{oc} \times FF / I_{Ins} \times 100 \quad (2)$$

Figure 5 shows the plot of the open-circuit potential versus short-circuit photocurrent density. The short-circuit photocurrent J_{sc} is obtained using the production and accumulation of light-generating carriers, while the sum of forward bias at the cell junction owing to the light-generating current provides open-circuit voltage, V_{oc} , for DSSCs. The fabricated DSSC photosensitized with *Alstroemeria* flower extracted dye demonstrated the highest V_{oc} (0.39 V), J_{sc} (2.04 mA/cm^2), FF (0.35), P_{max} (0.100 mW/cm^2) and high η (1.74%); while the fabricated solar cell photosensitized *Alpinia purpurata* extracted dye showed V_{oc} (0.53 V), J_{sc} (0.49 mA/cm^2), FF (0.40), P_{max} (0.280 mW) and η (0.65%). The adsorption of dye on the TiO_2 surface of the photoanode, the dye molecular structure, photosensitizers efficiency and the dye electron injection capability influence the sum of electrons that were photoexcited and, as a result, also influence the photocurrent densities of the fabricated DSSCs [48]. Excess molecules of dye adsorb on the surface of TiO_2 , which generates additional photons from sunlight, resulting in rapid electron injection. The primary elements that calculate the efficiency of DSSC are V_{oc} and J_{sc} . The open-circuit potential is the variation between the TiO_2 electrode Fermi level and redox electrolyte potential, which primarily depends on the rate of adsorption mode of the photosensitizer and recombination time [49,50]. Thus, the surface adsorption with *Alpinia purpurata* and *Alstroemeria* flower dyes as a photosensitizer plays a very significant function in DSSC fabrication [51–53]. Table 1 shows the comparative photovoltaic performances of natural dyes from previous literature. From the obtained results, it is evident that the *Alstroemeria* flower dyes showed higher efficiency compared to the other natural dyes, owing to the huge amount of cyanidin 3-glycosides molecule present in the extracted dye.

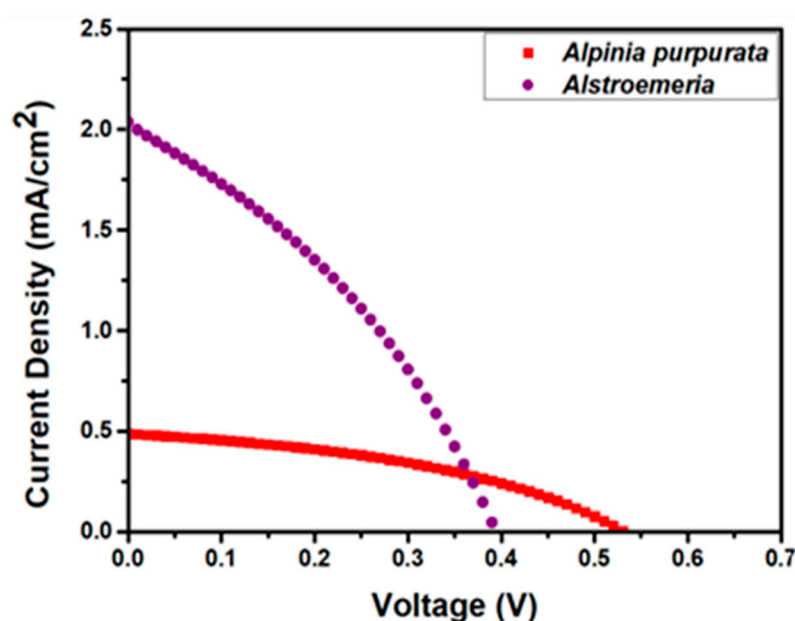
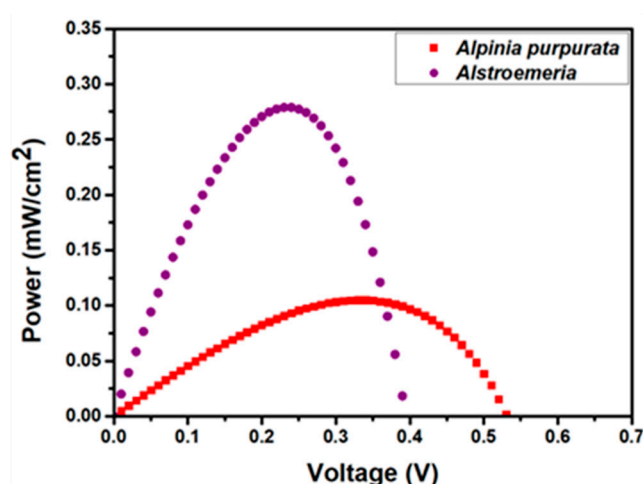


Figure 5. Photocurrent density vs. voltage profiles (J - V).

Table 1. Photovoltaic performances of DSSCs with various natural dyes compared with previous literature.

Dye	J_{sc} (mA/cm ²)	V_{oc} (V)	FF	η (%)	Ref.
<i>Jaboticaba</i>	0.38	0.41	0.29	0.13	[34]
<i>Thubergia Erecta</i>	0.27	0.54	0.08	0.38	[35]
<i>Achiote seeds</i>	1.1	0.57	0.59	0.37	[54]
<i>Henna</i>	0.42	0.54	0.38	0.09	[55]
<i>Sorghum Stem</i>	1.69	0.34	0.31	0.18	[56]
<i>Leucanthemum</i>	0.42	0.54	0.27	0.88	[37]
<i>Prickly Pear</i>	1.17	0.56	0.85	0.56	[57]
<i>Carica papaya</i>	1.77	0.40	0.42	0.29	[58]
<i>Chrysanthemum</i>	0.85	0.58	0.48	1.35	[59]
<i>Tropaeolum majus</i>	0.72	0.55	0.70	0.28	[60]
<i>Gerbera</i>	1.22	0.59	0.53	1.54	[41]
<i>Amaranthus cruentus</i>	5.81	0.49	0.28	0.81	[61]
<i>Areca catechu</i>	0.9	0.51	0.63	0.38	[62]
<i>Lantana repens</i>	0.45	0.69	0.34	0.12	[63]
<i>Solidago canadensis</i>	0.93	0.79	0.42	0.31	[63]
<i>Alstroemeria</i>	2.04	0.39	0.35	1.74	this work
<i>Alpinia purpurata</i>	0.49	0.53	0.40	0.65	this work

Figure 6 shows the power versus voltage (PV) curves for DSSCs based on *Alpinia purpurata* and *Alstroemeria* flower extracted dyes, and it can be applied to calculate the maximum power (P_{max}), which is attained by selecting a point from the obtained $J-V$ curve to the maximum photocurrent (J_{max}) and maximum potential (V_{max}). *Alpinia purpurata* and *Alstroemeria* flower extracted dyes demonstrate the power maximum P_{max} of 0.100 mW/cm² and 0.280 mW/cm², respectively. Figure 7a–d presents a comparative graph of the photoelectric components amongst the *Alpinia purpurata* and *Alstroemeria* flower extracted dyes-based DSSCs. The good performance obtained in this work was achieved with the DSSC photosensitized by *Alstroemeria*, reaching a yield (η) of 1.74%, obtaining a very satisfactory use in comparison with the sensitizer of *Alpinia purpurata* of 0.65%, as well as with some dyes used in the literature.

**Figure 6.** Power vs. voltage profiles ($P-V$).

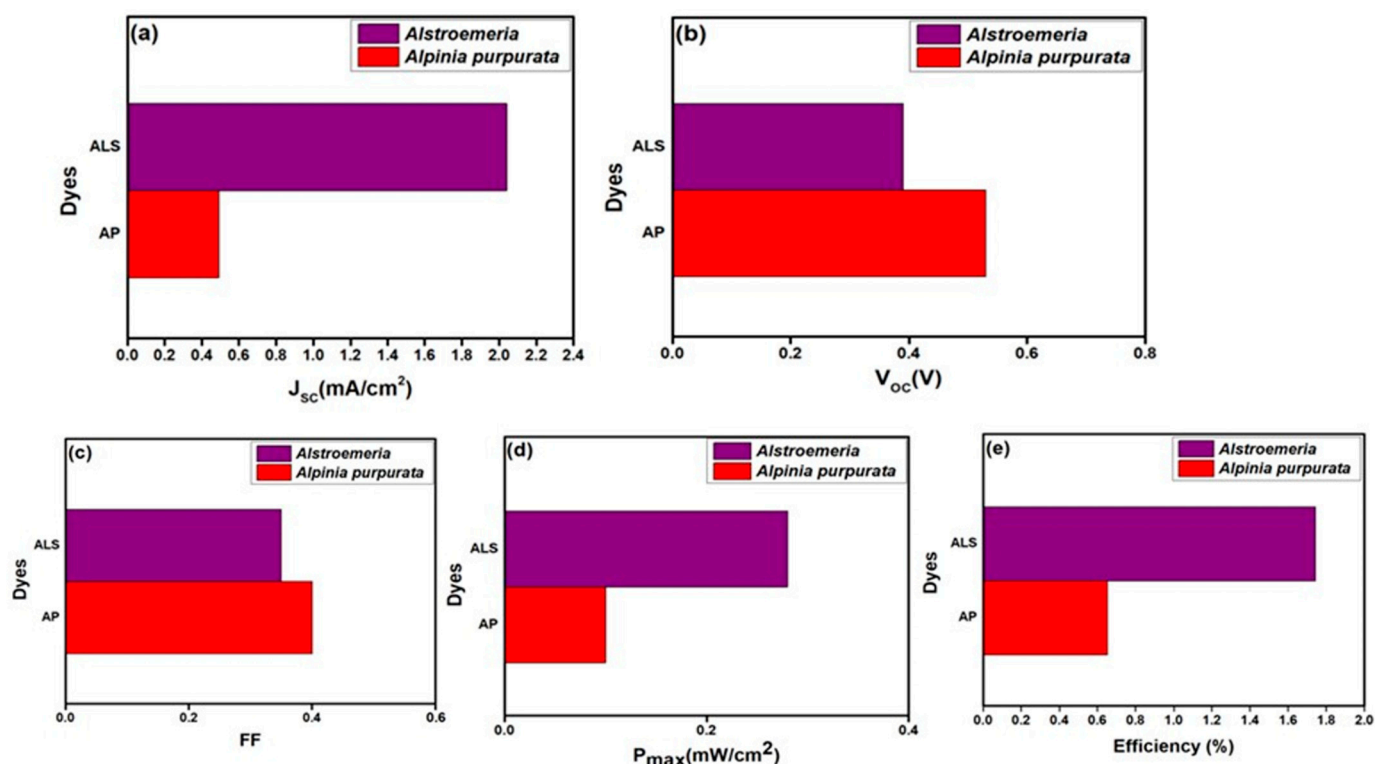


Figure 7. Comparative bar chart graphics of photoelectric components: (a) J_{sc} , (b) V_{oc} , (c) FF , (d) P_{max} and (e) η .

In order to evaluate the fabricated DSSC devices' internal impedances, electrochemical impedance spectroscopy (EIS) was performed, as demonstrated in Figure 8a. The EIS curves can be associated to the conductive film of FTO electrode substrate internal resistances, Pt counter electrode charge transfer, electrons transport at the interface of the photoanode surface (i.e., interfaces between the TiO_2 adsorbed photosensitizer and the redox electrolyte) and, in addition, recognition of the diffusion of the electrolyte process. Furthermore, all of these results of internal resistances sum up the internal resistance of the DSSC device [64–68]. An important technique to examine the impedance spectra is using fitting studies. This technique is likely to draw an equivalent circuit to study the electrochemical process, followed by executing a fitting of the theoretical components with the experimental results, thus resulting in original frequency response curves. The raw EIS results and the resultant equivalent circuits were obtained for *Alpinia purpurata* and *Alstroemeria* flower dyes-based DSSCs, as shown in Figure 8b. The obtained EIS fitting parameters and results were investigated and are summarized in Table 2. In a higher frequency range, a small semicircle was ascribed to the charge transfer resistances (R_1) of the redox electrolyte and Pt counter electrode (electrolyte/Pt), and the large semicircle in the lower frequency region was ascribed to the resistance for the charge transport of the dye-adsorbed TiO_2 and electrolyte (R_2) interface. The resistance of solution (R_s) corresponds to the electrolyte resistance and the substrate of FTO, whereas R_3 is attributed to electrolyte diffusion and serial ohmic resistance. Table 2 shows that the resistance values of low charge transfer result in the high short-circuit current density (J_{sc}) and efficiency (η), corroborating that the impedance values are low, which leads to high values of the DSSC total efficiency in *Alstroemeria* rather than *Alpinia purpurata*.

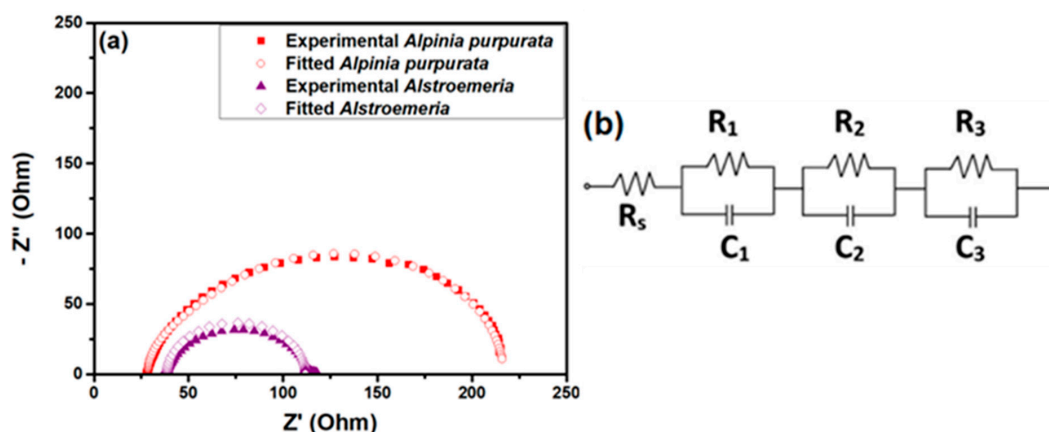


Figure 8. (a) DSSC device EIS spectra and (b) corresponding equivalent circuit.

Table 2. Equivalent circuit components with their related errors.

Dye	R_s (Ω)	R_1 (Ω)	R_2 (Ω)	R_3 (Ω)	C_1 (μF)	C_2 (μF)	C_3 (μF)
<i>Alpinia purpurata</i>	28.34	163.6	24.50	8.097	64.36	71.75	93.45
	± 0.53	± 1.50	± 9.85	± 8.26	± 3.63	± 4.15	± 5.29
<i>Alstroemeria</i>	38.56	73.16	15.75	6.017	44.29	144.28	87.43
	± 0.78	± 1.27	± 0.21	± 1.21	± 2.28	± 3.01	± 3.43

4. Conclusions

The novel dyes extracted from the petals of *Alstroemeria* and *Alpinia purpurata* flowers were used as photosensitizers in DSSC device construction. The identification of functional groups and electron excitation were established using FTIR and absorption spectroscopy, where it was possible to identify the existence of anthocyanin radicals (cyanidin 3-glycosides) in *Alstroemeria* and piperine in *Alpinia purpurata* flower extracts. Among these photosensitizers, the DSSC fabricated with flower petal extracts of *Alstroemeria* offered a noticeably high photoexcitation, good interaction with semiconductor oxide TiO_2 and good efficiency. The fabricated DSSC sensitized with *Alstroemeria* flower extract showed a high solar efficiency of 1.74% and P_{max} of $0.280 \text{ mW}/\text{cm}^2$, whereas the fabricated DSSC sensitized with *Alpinia purpurata* flower extracts showed a solar efficiency of $\sim 0.65\%$ and P_{max} of $0.100 \text{ mW}/\text{cm}^2$. The solar conversion efficiency might be enhanced through the introduction of ionic liquids-based redox electrolytes instead of organic electrolytes. Generally, the dyes extracted from natural species as photosensitizers of DSSCs construction are encouraging due to their biodegradability, low-cost, enhanced efficiency and renewability. It is concluded that the natural dyes used in this work in the development of DSSCs can be considered as good sensitizers, creating promising perspectives in the field of emerging solar cells.

Author Contributions: Conceptualization and methodology, L.R.B.d.C.; software, H.O.d.C.; validation, A.M.B.L.; writing—original draft preparation, R.S.B.; formal analysis, S.R.; visualization, C.R.; supervision and funding acquisition, A.L.F.d.B. All authors have read and agreed to the published version of the manuscript.

Funding: R.S. Babu would like to thank the Coordenação de Aperfeiçoamento de Pessoal de Nível Superior (CAPES) for the funding assistance (88887.798322/2022-00) and Fundação de Amparo à Pesquisa do Estado do Rio de Janeiro (FAPERJ) for the funding assistance of post-doctoral fellow senior (E-26/202.333/2021). A.L.F. de Barros would like to thank the Conselho Nacional de Desenvolvimento Científico e Tecnológico (CNPq) (307418/2021-9), Projeto Universal (407938/2018-4), Financiadora de Estudos e Projetos (FINEP) (0647/18), FAPERJ (210.965/2021, 210.801/2021, 245.307/2019 and 200.320/2023) for partial support. The students H.O. da Cunha and A.M.B. Leite wish to thank CAPES (001) for the financial assistance for their doctoral degree.

Institutional Review Board Statement: Not applicable.

Informed Consent Statement: Not applicable.

Data Availability Statement: Not applicable.

Acknowledgments: We are grateful to H.V. Rouco and N. Mangiavacchi from UERJ, Brazil, for helping with the FESEM measurements.

Conflicts of Interest: The authors declare no conflict of interest.

References

1. Bogdanov, D.; Ram, M.; Aghahosseini, A.; Gulagi, A.; Oyewo, A.S.; Child, M.; Caldera, U.; Sadovskaia, K.; Farfan, J.; Barbosa, L.D.S.N.S.; et al. Low-cost renewable electricity as the key driver of the global energy transition towards sustainability. *Energy* **2021**, *227*, 120467. [[CrossRef](#)]
2. Yashwantrao, G.; Saha, S. Perspective on the rational design strategies of quinoxaline derived organic sensitizers for dye-sensitized solar cells (DSSC). *Dyes Pigm.* **2022**, *199*, 110093. [[CrossRef](#)]
3. Kokkonen, M.; Talebi, P.; Zhou, J.; Asgari, S.; Soomro, S.A.; Elsehrawy, F.; Halme, J.; Ahmad, S.; Hagfeldt, A.; Hashmi, S.G. Advanced research trends in dye-sensitized solar cells. *J. Mater. Chem. A* **2021**, *9*, 10527–10545. [[CrossRef](#)]
4. O'Regan, B.; Grätzel, M. A low-cost, high-efficiency solar cell based on dye-sensitized colloidal TiO₂ films. *Nature* **1991**, *353*, 737–740. [[CrossRef](#)]
5. Maurya, I.C.; Singh, S.; Srivastava, P.; Maiti, B.; Bahadur, L. Natural dye extract from Cassia fistula and its application in dye-sensitized solar cell: Experimental and density functional theory studies. *Opt. Mater.* **2019**, *90*, 273–280. [[CrossRef](#)]
6. Noor, S.; Sajjad, S.; Leghari, S.A.K.; Shaheen, S.; Iqbal, A. ZnO/TiO₂ nanocomposite photoanode as an effective UV-Vis responsive dye sensitized solar cell. *Mater. Res. Express* **2018**, *5*, 095905. [[CrossRef](#)]
7. Grätzel, M. Dye-sensitized solar cells. *J. Photochem. Photobiol. C Photochem. Rev.* **2003**, *4*, 145–153. [[CrossRef](#)]
8. Hagfeldt, A.; Boschloo, G.; Sun, L.; Kloo, L.; Pettersson, H. Dye-sensitized solar cells. *Chem. Rev.* **2010**, *110*, 6595–6663. [[CrossRef](#)]
9. Amao, Y.; Komori, T. Bio-photovoltaic conversion device using chlorine-e₆ derived from chlorophyll from *Spirulina* adsorbed on a nanocrystalline TiO₂ film electrode. *Biosens. Bioelectron.* **2004**, *19*, 843–847. [[CrossRef](#)]
10. Ludin, N.A.; Mahmoud, A.M.A.-A.; Mohamad, A.B.; Kadhun, A.A.H.; Sopian, K.; Karim, N.S.A. Review on the development of natural dye photosensitizer for dye-sensitized solar cells. *Renew. Sust. Energy Rev.* **2014**, *31*, 386–396. [[CrossRef](#)]
11. Hao, S.; Wu, J.; Huang, Y.; Lin, J. Natural dyes as photosensitizers for dye-sensitized solar cell. *Sol. Energy* **2006**, *80*, 209–214. [[CrossRef](#)]
12. Polo, A.S.; Iha, N.Y.M. Blue sensitizers for solar cells: Natural dyes from Calafate and Jaboticaba. *Sol. Energy Mater. Sol. Cells* **2006**, *90*, 1936–1944. [[CrossRef](#)]
13. Zainudin, S.N.F.; Abdullah, H.; Markom, M. Electrochemical studies of tin oxide based-dye-sensitized solar cells (DSSC): A review. *J. Mater. Sci. Mater. Electron.* **2019**, *30*, 5342–5356. [[CrossRef](#)]
14. Garcia-Salinas, M.J.; Ariza, M.J. Optimizing a simple natural dye production method for dye-sensitized solar cells: Examples for Betalain (Bougainvillea and Beetroot Extracts) and anthocyanin dyes. *Appl. Sci.* **2019**, *9*, 2515. [[CrossRef](#)]
15. Ambapuram, M.; Maddala, G.; Simhachalam, N.B.; Sripada, S.; Kalvapalli, S.; Pedda, V.S.Y.; Mitty, R. Highly effective SnS composite counter electrode sandwiched bi-function CeO₂:Er³⁺/Yb³⁺ assisted surface modified photoelectrode dye sensitized solar cell exceeds 9.5% efficiency. *Sol. Energy* **2020**, *207*, 1158–1164. [[CrossRef](#)]
16. Mathew, S.; Ganguly, P.; Rhatigan, S.; Kumaravel, V.; Byrne, C.; Hinder, S.J.; Bartlett, J.; Nolan, M.; Pillai, S.C. Cu-doped TiO₂: Visible light assisted photocatalytic antimicrobial activity. *Appl. Sci.* **2018**, *8*, 2067. [[CrossRef](#)]
17. Subalakshmi, K.; Senthilselvan, J. Effect of fluorine-doped TiO₂ photoanode on electron transport, recombination dynamics and improved DSSC efficiency. *Sol. Energy* **2018**, *171*, 914–928. [[CrossRef](#)]
18. Langmar, O.; Fazio, E.; Schol, P.; de la Torre, G.; Costa, R.D.; Torres, T.; Guldi, D.M. Controlling interfacial charge transfer and fill factors in CuO-based tandem dye-sensitized solar cells. *Angew. Chem. Int. Ed.* **2019**, *58*, 4056–4060. [[CrossRef](#)]
19. Samanta, P.N.; Majumdar, D.; Roszak, S.; Leszczynski, J. First-principles approach for assessing cold electron injection efficiency of dye-sensitized solar cell: Elucidation of mechanism of charge injection and recombination. *J. Phys. Chem. C* **2020**, *124*, 2817–2836. [[CrossRef](#)]
20. Shanmugam, V.; Manoharan, S.; Anandan, S.; Murugan, R. Performance of dye-sensitized solar cells fabricated with extracts from fruits of ivy gourd and flowers of red frangipani as sensitizers. *Spectrochim. Acta Part A* **2013**, *104*, 35–40. [[CrossRef](#)]
21. Kimpa, M.I.; Momoh, M.; Isah, K.U.; Yahya, H.N.; Ndamitso, M.M. Photoelectric characterization of dye sensitized solar cells using natural dye from pawpaw leaf and flame tree flower as sensitizers. *Mater. Sci. Appl.* **2012**, *3*, 281–286.
22. Maabong, K.; Muiva, C.M.; Monowe, P.; Sathiaraj, S.T.; Hopkins, M.; Nguyen, L.; Malungwa, K.; Thobega, M. Natural pigments as photosensitizers for dye-sensitized solar cells with TiO₂ thin films. *Int. J. Renew. Energy Res.* **2015**, *5*, 54–60.
23. Teoli, F.; Lucioli, S.; Nota, O.; Frattarelli, A.; Matteocci, F.; Di Carlo, A.; Caboni, E.; Forni, C. Role of pH and pigment concentration for natural dye-sensitized solar cells treated with anthocyanin extracts of common fruits. *J. Photochem. Photobiol. A Chem.* **2016**, *316*, 24–30. [[CrossRef](#)]

24. Calogero, G.; Marco, G.D. Red Sicilian orange and purple eggplant fruits as natural sensitizers for dye-sensitized solar cells. *Sol. Energy Mater. Sol. Cells* **2008**, *92*, 1341–1346. [[CrossRef](#)]
25. Chang, H.; Lo, Y.J. Pomegranate leaves and mulberry fruit as natural sensitizers for dye-sensitized solar cells. *Sol. Energy* **2010**, *84*, 1833–1837. [[CrossRef](#)]
26. Mozaffari, S.A.; Saeidi, M.; Rahmani, R. Photoelectric characterization of fabricated dye-sensitized solar cell using dye extracted from red Siahkooti fruit as natural sensitizer. *Spectrochim. Acta Part A* **2015**, *142*, 226–231. [[CrossRef](#)]
27. Singh, L.K.; Karlo, T.; Pandey, A. Performance of fruit extract of *Melastoma malabathricum* L. as sensitizer in DSSCs. *Spectrochim. Acta Part A* **2014**, *118*, 938–943. [[CrossRef](#)]
28. Calogero, G.; Marco, G.D.; Cazzanti, S.; Caramori, S.; Argazzi, R.; Carlo, A.D.; Bignozzi, C.A. Efficient dye-sensitized solar cells using red turnip and purple wild sicilian prickly pear fruits. *Int. J. Mol. Sci.* **2010**, *11*, 254–267. [[CrossRef](#)]
29. Rosana, N.T.M.; Amarnath, D.J.; Joseph, K.L.V.; Anandan, S. Mixed dye from nerium oleander and hibiscus flowers as a photo sensitizer in dye sensitized solar cells. *Int. J. Chem. Tech. Res.* **2014**, *6*, 5022–5026.
30. Tian, H.; Chen, K.; Ye, X.; Yang, S.; Gu, Q. Hydrothermal growth of $\text{Bi}_2\text{Ti}_2\text{O}_7/\text{TiO}_2$ and $\text{Bi}_4\text{Ti}_3\text{O}_{12}/\text{TiO}_2$ heterostructures on highly ordered TiO_2 -nanotube arrays for dye-sensitized solar cells. *Ceram. Int.* **2019**, *45*, 20750–20757. [[CrossRef](#)]
31. Idris, A.; Linatoc, A.C.; Bakar, M.F.A.; Takai, Z.I.; Audu, Y. Effect of light quality and quantity on the accumulation of flavonoid in plant species. *J. Sci. Technol.* **2018**, *10*, 32–45. [[CrossRef](#)]
32. Yousefi, F.; Jabbarzadeh, Z.; Amiri, J.; Rasouli-Sadaghiani, M.; Shaygan, A. Foliar application of polyamines improve some morphological and physiological characteristics of rose. *Folia Hortic.* **2021**, *33*, 147–156. [[CrossRef](#)]
33. Tomar, N.; Agrawal, A.; Dhaka, V.S.; Surolia, P.K. Ruthenium complexes based dye sensitized solar cells: Fundamentals and research trends. *Sol Energy* **2020**, *207*, 59–76. [[CrossRef](#)]
34. Sampaio, D.M.; Babu, R.S.; Costa, H.R.M.; de Barros, A.L.F. Investigation of nanostructured TiO_2 thin film coatings for DSSCs application using natural dye extracted from jabuticaba fruit as photosensitizers. *Ionic* **2019**, *25*, 2893–2902. [[CrossRef](#)]
35. Ferreira, B.C.; Sampaio, D.M.; Babu, R.S.; de Barros, A.L.F. Influence of nanostructured TiO_2 film thickness in dye-sensitized solar cells using naturally extracted dye from *Thunbergia erecta* flowers as a photosensitizer. *Opt. Mater.* **2018**, *86*, 239–246. [[CrossRef](#)]
36. Karim, N.A.; Mehmood, U.; Zahid, H.F.; Asi, T. Nanostructured photoanode and counter electrode materials for efficient Dye-Sensitized Solar Cells (DSSCs). *Sol. Energy* **2019**, *185*, 165–188. [[CrossRef](#)]
37. Ferreira, F.C.; Babu, R.S.; de Barros, A.L.F.; Raja, S.; da Conceição, L.R.B.; Mattoso, L.H.C. Photoelectric performance evaluation of DSSCs using the dye extracted from different color petals of *Leucanthemum vulgare* flowers as novel sensitizers. *Spectrochim. Acta A* **2020**, *233*, 118198. [[CrossRef](#)]
38. Kuppu, S.V.; Jeyaraman, A.R.; Guruviah, P.K.; Thambusamy, S. Preparation and characterizations of PMMA-PVDF based polymer composite electrolyte materials for dye sensitized solar cell. *Curr. Appl. Phys.* **2018**, *18*, 619–625. [[CrossRef](#)]
39. Fang, Y.; Ma, P.; Cheng, H.; Tan, G.; Wu, J.; Zheng, J.; Zhou, X.; Fang, S.; Dai, Y.; Lin, Y. Synthesis of low-viscosity ionic liquids for application in dye-sensitized solar cells. *Chem. Asian J.* **2019**, *14*, 4201–4206. [[CrossRef](#)]
40. Cheng, F.; Wu, C.; Wang, S.; Wen, S. Polydopamine-modified electrospun polyvinylidene fluoride nanofiber based flexible polymer gel electrolyte for highly stable dye-sensitized solar cells. *ACS Omega* **2021**, *6*, 28663–28670. [[CrossRef](#)]
41. dos Santos, F.M.M.; Leite, A.M.B.; da Conceição, L.R.B.; Sasikumar, Y.; Atchudan, R.; Pinto, M.F.; Babu, R.S.; de Barros, A.L.F. Effect of bandgap energies by various color petals of *Gerbera Jamesonii* flower dyes as a photosensitizer on enhancing the efficiency of dye-sensitized solar cells. *J. Mater. Sci. Mater. Electron.* **2022**, *33*, 20338–20352. [[CrossRef](#)]
42. Lee, K.E.; Gomez, M.A.; Elouatik, S.; Demopoulos, G.P. Further understanding of the adsorption mechanism of N719 sensitizer on anatase TiO_2 Films for DSSC applications using vibrational spectroscopy and confocal Raman imaging. *Langmuir* **2010**, *26*, 9575–9583. [[CrossRef](#)] [[PubMed](#)]
43. Hospodarova, V.; Singovszka, E.; Stevulova, N. Characterization of cellulosic fibers by FTIR spectroscopy for their further implementation to building materials. *Am. J. Anal. Chem.* **2018**, *9*, 303–310. [[CrossRef](#)]
44. Akila, Y.; Muthukumarasamy, N.; Agilan, S.; Mallick, T.K.; Senthilarasu, S.; Velauthapillai, D. Enhanced performance of natural dye sensitized solar cells fabricated using rutile TiO_2 nanorods. *Opt. Mater.* **2016**, *58*, 76–83. [[CrossRef](#)]
45. Sirat, H.M.; Liamen, M.R. Chemical constituents of *Alpinia purpurata*. *Pertanika J. Sci. Technol.* **1995**, *3*, 67–71.
46. Patni, N.; Pillai, S.G.; Sharma, P. Effect of using betalain, anthocyanin and chlorophyll dyes together as a sensitizer on enhancing the efficiency of dye sensitized solar cell. *Int. J. Energy Res.* **2020**, *44*, 10846–10859. [[CrossRef](#)]
47. Pathak, C.; Surana, K.; Shukla, V.K.; Singh, P.K. Fabrication and characterization of dye sensitized solar cell using natural dyes. *Mater. Today Proc.* **2019**, *12*, 665–670.
48. Krebs, F.C. Fabrication and processing of polymer solar cells: A review of printing and coating techniques. *Sol. Energy Mater. Sol. Cells* **2009**, *93*, 394–412. [[CrossRef](#)]
49. Das, A.; Nair, R.G. Fabrication of In_2O_3 functionalized ZnO based nano heterojunction photoanode for improved DSSC performance through effective interfacial charge carrier separation. *Opt. Mater.* **2021**, *122 Pt B*, 111784. [[CrossRef](#)]
50. Jose, R.; Thavasi, V.; Ramakrishna, S. Metal oxides for dye-sensitized solar cells. *J. Am. Ceram. Soc.* **2009**, *92*, 289–301. [[CrossRef](#)]
51. de Angelis, F.; Fantacci, S.; Selloni, A.; Gratzel, M.; Nazeeruddin, M.K. Influence of the sensitizer adsorption mode on the open-circuit potential of dye-sensitized solar cells. *Nano Lett.* **2007**, *7*, 3189–3195. [[CrossRef](#)] [[PubMed](#)]
52. Meng, S.; Ren, J.; Kaxiras, E. Natural Dyes Adsorbed on TiO_2 Nanowire for photovoltaic applications: Enhanced light absorption and ultrafast electron injection. *Nano Lett.* **2008**, *8*, 3266–3272. [[CrossRef](#)] [[PubMed](#)]

53. Yamazaki, E.; Murayama, M.; Nishikawa, N.; Hashimoto, N.; Shoyama, M.; Kurita, O. Utilization of natural carotenoids as photosensitizers for dye-sensitized solar cells. *Sol. Energy* **2007**, *81*, 512–516. [[CrossRef](#)]
54. Gómez-Ortíz, N.M.; Vázquez-Maldonado, I.A.; Pérez-Espadas, A.R.; Mena-Rejón, G.J.; Azamar-Barrios, J.A.; Oskam, G. Dye-sensitized solar cells with natural dyes extracted from achiote seeds. *Sol. Energy Mater. Sol. Cells* **2010**, *94*, 40–44. [[CrossRef](#)]
55. Sowmya, S.; Prakash, P.; Ruba, N.; Janarthanan, B.; Prabu, A.N.; Chandrasekaran, J. A study on the fabrication and characterization of dye-sensitized solar cells with *Amaranthus red* and *Lawsonia inermis* as sensitizers with maximum absorption of visible light. *J. Mater. Sci. Mater. Electron.* **2020**, *31*, 6027–6035. [[CrossRef](#)]
56. Sanda, M.D.A.; Badu, M.; Awudza, J.A.M.; Boadi, N.O. Development of TiO₂-based dye-sensitized solar cells using natural dyes extracted from some plant-based materials. *Chem. Int.* **2021**, *7*, 9–20.
57. Purushothamreddy, N.; Dileep, R.K.; Veerappan, G.; Kovendhan, M.; Joseph, D.P. Prickly pear fruit extract as photosensitizer for dye-sensitized solar cell. *Spectrochim. Acta A* **2020**, *228*, 117686. [[CrossRef](#)]
58. Ossai, A.N.; Ezike, S.C.; Timtere, P.; Ahmed, A.D. Enhanced photovoltaic performance of dye-sensitized solar cells-based Carica papaya leaf and black cherry fruit co-sensitizers. *Chem. Phys. Impact* **2021**, *2*, 100024. [[CrossRef](#)]
59. Leite, A.M.B.; da Cunha, H.O.; Rodrigues, J.A.F.C.R.; Babu, R.S.; de Barros, A.L.F. Construction and characterization of organic photovoltaic cells sensitized by Chrysanthemum based natural dye. *Spectrochim. Acta A* **2023**, *284*, 121780. [[CrossRef](#)]
60. Singh, S.; Maurya, I.C.; Sharma, S.; Kushwaha, P.S.; Srivastava, P.; Bahadur, L. Application of new natural dyes extracted from Nasturtium flowers (*Tropaeolum majus*) as photosensitizer in dye-sensitized solar cells. *Optik* **2021**, *243*, 167331. [[CrossRef](#)]
61. Sankaranarayanan, S.; Kathiravan, I.; Balasundaram, J.; Shkir, M.; Alfaify, S. An analysis of the dye-sensitized solar cells fabricated with the dyes extracted from the leaves and flowers of *Amaranthus cruentus*. *Environ. Sci. Poll. Res.* **2022**, *29*, 44271–44281. [[CrossRef](#)] [[PubMed](#)]
62. Al-Alwani, M.A.M.; Hassimi, A.H.; Al-Shorgani, N.K.N.; Al-Mashaan, A.B.S.A. Natural dye extracted from *Areca catechu* fruits as a new sensitizer for dye-sensitized solar cell fabrication: Optimization using D-Optimal design. *Mater. Chem. Phys.* **2020**, *240*, 122204. [[CrossRef](#)]
63. Ferreira, B.C.; Babu, R.S.; da Conceição, L.R.B.; da Cunha, H.O.; Sampaio, D.M.; Samyn, L.M.; de Barros, A.L.F. Performance evaluation of DSSCs using naturally extracted dyes from petals of *Lantana repens* and *Solidago canadensis* flowers as light-harvesting units. *Ionics* **2022**, *28*, 5233–5242. [[CrossRef](#)]
64. Rudra, S.; Seo, H.W.; Sarker, S.; Kim, D.M. Simulation and electrochemical impedance spectroscopy of dye-sensitized solar cells. *J. Indus. Eng. Chem.* **2021**, *97*, 574–583. [[CrossRef](#)]
65. Sinha, D.; De, D.; Ayaz, A. Photo sensitizing and electrochemical performance analysis of mixed natural dye and nanostructured ZnO based DSSC. *Sādhanā* **2020**, *45*, 175. [[CrossRef](#)]
66. Chou, J.C.; Lu, C.C.; Liao, Y.H.; Lai, C.H.; Nien, Y.H.; Kuo, C.H.; Ko, C.C. Fabrication and electrochemical impedance analysis of dye-sensitized solar cells with titanium dioxide compact layer and graphene oxide dye absorption layer. *IEEE Trans. Nanotechnol.* **2019**, *18*, 461–466. [[CrossRef](#)]
67. Faraz, S.M.; Mazhar, M.; Shah, W.; Noor, H.; Awan, Z.H.; Sayyad, M.H. Comparative study of impedance spectroscopy and photovoltaic properties of metallic and natural dye based dye sensitized solar cells. *Phys. B Condens. Matter* **2021**, *602*, 412567. [[CrossRef](#)]
68. da Conceição, L.R.B.; de Barros, A.L.F.; Haddad, D.B.; Babu, R.S. *Passiflora edulis* and *Cocos nucifera* extracts as light-harvesters for efficient dye-sensitized solar cells. In Proceedings of the 2020 IEEE ANDESCON, Quito, Ecuador, 13–16 October 2020; pp. 1–5.

Disclaimer/Publisher’s Note: The statements, opinions and data contained in all publications are solely those of the individual author(s) and contributor(s) and not of MDPI and/or the editor(s). MDPI and/or the editor(s) disclaim responsibility for any injury to people or property resulting from any ideas, methods, instructions or products referred to in the content.